

# High-resolution FTIR spectrum and analysis of the $\nu_2 + \nu_4$ combination band of $^{32}\text{SF}_6$

V. Boudon<sup>a,\*</sup> and N. Lacome<sup>b</sup>

<sup>a</sup> *Laboratoire de Physique de l'Université de Bourgogne, CNRS UMR 5027, 9, Avenue Alain Savary, BP 47870, F-21078 Dijon Cedex, France*

<sup>b</sup> *Laboratoire de Dynamique, Interactions et Réactivité, CNRS UMR 7075, Case 49, Université Paris 6, 4 Place Jussieu, F-75252 Paris Cedex 05, France*

Received 22 July 2003; in revised form 27 August 2003

## Abstract

The spectroscopic knowledge of sulfur hexafluoride, which is necessary for a correct remote sensing and monitoring of this species in the Earth's atmosphere, is still very partial. In particular, the hot bands in the strongly absorbing  $\nu_3$  region (near  $948\text{ cm}^{-1}$ ) have not been analyzed yet. Their study implies the analysis of many vibrational levels and thus the spectroscopy of various fundamental, harmonic, and combination bands. The present work is a new contribution to this topic, concerning the  $\nu_2 + \nu_4$  combination band. The FTIR spectrum of this region has been recorded at room temperature with a resolution of  $0.002\text{ cm}^{-1}$ . The data have been analyzed thanks to the HTDS software (<http://www.u-bourgogne.fr/LPUB/shTDS.html>) developed in Dijon for  $\text{XY}_6$  octahedral molecules. Seven hundred and fifty-nine lines could be assigned up to  $J = 112$ , and the standard deviation is  $0.0022\text{ cm}^{-1}$ . The distance between the two vibrational sublevels with respective symmetry  $F_{1u}$  and  $F_{2u}$  is  $0.348\text{ cm}^{-1}$ .

© 2003 Elsevier Inc. All rights reserved.

**Keywords:** Sulfur hexafluoride; High resolution; Combination band

## 1. Introduction

Sulfur hexafluoride appears to be a species of growing importance in the field of atmospheric physics and chemistry [1] as a pollutant that can contribute to the greenhouse effect [2,3].  $\text{SF}_6$  concentration in the Earth's atmosphere is increasing at a rate of about 7% per year due to industrial emissions and this very inert molecule has an extremely long lifetime in the atmosphere (ca. 3200 years) [4,5].  $\text{SF}_6$  is included as one of the species to control in the Kyoto protocol [6–8].

However, as we have shown in a recent review article [9] and in previous papers [10–13], the spectroscopy of this molecule, which is essential for quantitative measurements in the atmosphere, is still insufficiently known. In particular, the region of the  $\nu_3$  fundamental

near  $948\text{ cm}^{-1}$  is of primary importance since its very strong absorption is responsible for the huge greenhouse capabilities of  $\text{SF}_6$ . Although the  $\nu_3 = 1$  level itself is very well known [14], the hot bands in this region which largely contribute to the absorption (the ground state population is only 30% at 300 K [9]) are very poorly known. The study of these hot bands requires the investigation of many vibrational bands, including fundamentals, combinations, and harmonics.

The present paper is a new contribution to this topic concerning  $\nu_2 + \nu_4$ . We have recorded a high-resolution Fourier transform infrared (FTIR) spectrum of this combination band and analyzed it up to very high-rotational quantum number values ( $J$  up to 112). The only existing study concerning  $\nu_2 + \nu_4$  was reported in 1986 by McDowell et al. [15] using a very approximate model which considered only the  $F_{1u}$  sublevel; this is not sufficient to interpret the high-resolution spectrum in detail. The analysis presented here has been performed using the HTDS program suite [16].

\* Corresponding author. Fax: +33-3-80-39-59-71.

E-mail addresses: [Vincent.Boudon@u-bourgogne.fr](mailto:Vincent.Boudon@u-bourgogne.fr) (V. Boudon), [lacome@glvt-cnrs.fr](mailto:lacome@glvt-cnrs.fr) (N. Lacome).

## 2. Experiment

Spectra of pure SF<sub>6</sub> in the spectral region ranging from 500 to 2000 cm<sup>-1</sup> have been recorded using a Bruker IFS 120 FTIR spectrometer. The recorded region contained several transitions and, as a first step, we focused on the  $\nu_2 + \nu_4$  transition. The spectrometer was equipped with a KBr/Ge beamsplitter, a SiC source and a photovoltaic MCT detector. It was continuously evacuated to obtain a working residual pressure around  $8 \times 10^{-3}$  mbar and the whole optical path was maintained under vacuum. A white-type cell, equipped with CaF<sub>2</sub> windows, allowed an optical path of 4.15 m. The SF<sub>6</sub> sample, 99.97% pure, was supplied by “Alpha Gaz,” a division of “L’Air Liquide” and used without any further purification. Pressures were measured with capacitance gauges and temperatures were continuously monitored using four 100  $\Omega$ -platinum sensors set up inside the cell. Three spectra were recorded for pressures equal to 6.894, 10.371, and 19.78 mbar, respectively, all at room temperature and under 0.002 cm<sup>-1</sup> resolution. A particular procedure was used for improving the quality of these spectra. Every recorded interferogram, corresponding to one scan of the mobile mirror, was phase corrected, Fourier transformed and stored. Then, the individual spectra were averaged without any weighting procedure. The three final spectra all correspond to 140 scans. Fig. 1 shows an overview of the  $\nu_2 + \nu_4$  absorption spectrum.

## 3. Theoretical model

The theoretical model used in this paper is based on the tensorial formalism and the vibrational extrapolation methods developed in Dijon. These methods have already been explained for example in [17,18]. If we consider an XY<sub>6</sub> molecule for which the vibrational levels are grouped in a series of polyads designed by

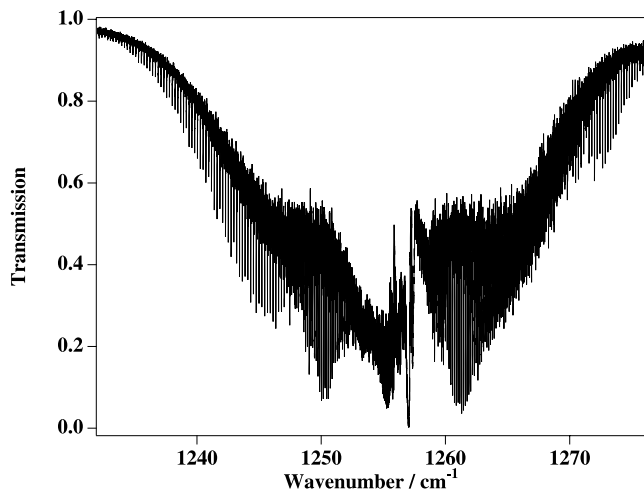


Fig. 1. Overview of the FTIR spectrum of  $\nu_2 + \nu_4$ .

$P_k$  ( $k = 0, \dots, n$ ),  $P_0$  being the ground state (GS), the Hamiltonian operators can be put in the following form (after performing some contact transformations):

$$\mathcal{H} = \mathcal{H}_{\{P_0 \equiv GS\}} + \mathcal{H}_{\{P_1\}} + \dots + \mathcal{H}_{\{P_n\}}, \quad (1)$$

where the  $\mathcal{H}_{\{P_k\}}$  contain rovibrational operators which have no matrix elements within the  $P_{k' < k}$  basis sets. The different terms are written in the form

$$\mathcal{H}_{\{P_k\}} = \sum_{\text{all indexes}} t_{\{s\}\{s'\}}^{\Omega(K,n\Gamma)\Gamma_v\Gamma_{v'}} T_{\{s\}\{s'\}}^{\Omega(K,n\Gamma)\Gamma_v\Gamma_{v'}}. \quad (2)$$

In this equation the  $t_{\{s\}\{s'\}}^{\Omega(K,n\Gamma)\Gamma_v\Gamma_{v'}}$  term is the parameter and  $T_{\{s\}\{s'\}}^{\Omega(K,n\Gamma)\Gamma_v\Gamma_{v'}}$  the rovibrational operator defined as

$$T_{\{s\}\{s'\}}^{\Omega(K,n\Gamma)\Gamma_v\Gamma_{v'}} = \beta \left[ \epsilon V_{\{s\}\{s'\}}^{\Gamma_v\Gamma_{v'}(\Gamma)} \otimes R^{\Omega(K,n\Gamma)} \right]^{(A_{1g})}, \quad (3)$$

where  $\beta$  is numerical factor equal to  $\sqrt{3}(-\sqrt{3}/4)^{\Omega/2}$  if  $(K, n\Gamma) = (0, 0A_1)$ , and equal to 1 otherwise. As shown by Eq. (3), the rovibrational operators  $T_{\{s\}\{s'\}}^{\Omega(K,n\Gamma)\Gamma_v\Gamma_{v'}}$  are obtained by coupling of a rotational operator  $R^{\Omega(K,n\Gamma)}$  of degree  $\Omega$  (in the angular momentum components  $J_x$ ,  $J_y$  or  $J_z$ ) and a vibrational operator  $\epsilon V_{\{s\}\{s'\}}^{\Gamma_v\Gamma_{v'}(\Gamma)}$  of degree  $\Omega_v$  (in creation or annihilation operators). The order of each individual term is  $\Omega + \Omega_v - 2$ .

The effective Hamiltonian for polyad  $P_n$  is obtained by projecting  $\mathcal{H}$  in the  $P_n$  Hilbert subspace, i.e.,

$$\begin{aligned} H^{(P_n)} &= P^{(P_n)} \mathcal{H} P^{(P_n)} \\ &= H_{\{GS\}}^{(P_n)} + \dots + H_{\{P_k\}}^{(P_n)} + \dots + H_{\{P_n\}}^{(P_n)}. \end{aligned} \quad (4)$$

In order to analyze the  $\nu_2 + \nu_4$  Raman spectra, we need the following effective Hamiltonians:

$$\tilde{H}^{(GS)} = \tilde{H}_{\{GS\}}^{(GS)}, \quad (5)$$

(the ground state effective Hamiltonian) and

$$\tilde{H}^{(\nu_2+\nu_4)} = \tilde{H}_{\{GS\}}^{(\nu_2+\nu_4)} + \tilde{H}_{\{\nu_2\}}^{(\nu_2+\nu_4)} + \tilde{H}_{\{\nu_4\}}^{(\nu_2+\nu_4)} + \tilde{H}_{\{\nu_2+\nu_4\}}^{(\nu_2+\nu_4)}, \quad (6)$$

(the  $\nu_2 = \nu_4 = 1$  effective Hamiltonian).

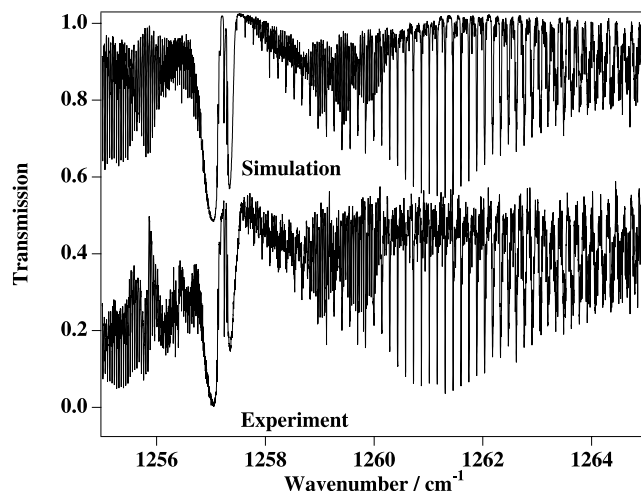


Fig. 2. Comparison between experimental and simulated spectra in the Q branches region.

Table 1  
Effective Hamiltonian parameters for the  $v_2 + v_4$  band of  $^{32}\text{SF}_6$

Order in $\tilde{H}$	Parameter $\Omega(K,n\Gamma)F_v\Gamma'_v$ $I_{(s)}\{s'\}$			Value ( $\text{cm}^{-1}$ )	“Usual notation”
	$\Omega(K, n\Gamma)$	$\{s\}\Gamma_v$	$\{s'\}\Gamma'_v$		
<i>Ground state</i>					
0	2(0, 0A <sub>1g</sub> )	000000A <sub>1g</sub>	000000A <sub>1g</sub>	$9.1078389192 \times 10^{-2a}$	$B_0$
2	4(0, 0A <sub>1g</sub> )	000000A <sub>1g</sub>	000000A <sub>1g</sub>	$-6.3369998149 \times 10^{-9a}$	$-D_0$
	4(4, 0A <sub>1g</sub> )	000000A <sub>1g</sub>	000000A <sub>1g</sub>	$1.8196943510 \times 10^{-10a}$	
4	6(0, 0A <sub>1g</sub> )	000000A <sub>1g</sub>	000000A <sub>1g</sub>	$-1.5890094350 \times 10^{-13a}$	
	6(4, 0A <sub>1g</sub> )	000000A <sub>1g</sub>	000000A <sub>1g</sub>	$1.0083389785 \times 10^{-14a}$	
	6(6, 0A <sub>1g</sub> )	000000A <sub>1g</sub>	000000A <sub>1g</sub>	$-1.0615255469 \times 10^{-16a}$	
6	8(0, 0A <sub>1g</sub> )	000000A <sub>1g</sub>	000000A <sub>1g</sub>	$5.9060087823 \times 10^{-19a}$	
	8(4, 0A <sub>1g</sub> )	000000A <sub>1g</sub>	000000A <sub>1g</sub>	$6.5795734511 \times 10^{-20a}$	
	8(6, 0A <sub>1g</sub> )	000000A <sub>1g</sub>	000000A <sub>1g</sub>	$-8.9391941374 \times 10^{-21a}$	
	8(8, 0A <sub>1g</sub> )	000000A <sub>1g</sub>	000000A <sub>1g</sub>	$-9.6703402824 \times 10^{-22a}$	
$v_2 = 1$					
0	0(0, 0A <sub>1g</sub> )	010000E <sub>g</sub>	010000E <sub>g</sub>	$0.64337444254 \times 10^{+3a}$	$v_2$
2	2(0, 0A <sub>1g</sub> )	010000E <sub>g</sub>	010000E <sub>g</sub>	$0.15925303267 \times 10^{-4a}$	$B_2 - B_0$
	2(2, 0E <sub>g</sub> )	010000E <sub>g</sub>	010000E <sub>g</sub>	$0.31554501045 \times 10^{-4a}$	
3	3(3, 0A <sub>2g</sub> )	010000E <sub>g</sub>	010000E <sub>g</sub>	$-0.14349111424 \times 10^{-7a}$	
$v_4 = 1$					
0	0(0, 0A <sub>1g</sub> )	000100F <sub>1u</sub>	000100F <sub>1u</sub>	$0.61498196293 \times 10^{+3a}$	$v_4$
1	1(1, 0F <sub>1g</sub> )	000100F <sub>1u</sub>	000100F <sub>1u</sub>	$-0.83691354775 \times 10^{-1a}$	$3\sqrt{2}(B\zeta)_4$
2	2(0, 0A <sub>1g</sub> )	000100F <sub>1u</sub>	000100F <sub>1u</sub>	$-0.19670143352 \times 10^{-4a}$	$B_4 - B_0$
	2(2, 0E <sub>g</sub> )	000100F <sub>1u</sub>	000100F <sub>1u</sub>	$0.10265400000 \times 10^{-4a}$	
	2(2, 0F <sub>2g</sub> )	000100F <sub>1u</sub>	000100F <sub>1u</sub>	$-0.16680802563 \times 10^{-4a}$	
3	3(1, 0F <sub>1g</sub> )	000100F <sub>1u</sub>	000100F <sub>1u</sub>	$-0.33454281827 \times 10^{-7a}$	
	3(3, 0F <sub>1g</sub> )	000100F <sub>1u</sub>	000100F <sub>1u</sub>	$0.17115870822 \times 10^{-7a}$	
4	4(0, 0A <sub>1g</sub> )	000100F <sub>1u</sub>	000100F <sub>1u</sub>	$-0.19318206570 \times 10^{-10a,b}$	$-(D_4 - D_0)$
$v_2 = v_4 = 1: F_{1u}$ sublevel					
2	0(0, 0A <sub>1g</sub> )	010100F <sub>1u</sub>	010100F <sub>1u</sub>	$-0.134301(36)$	
3	1(1, 0F <sub>1g</sub> )	010100F <sub>1u</sub>	010100F <sub>1u</sub>	$-0.2237(26) \times 10^{-2}$	
4	2(0, 0A <sub>1g</sub> )	010100F <sub>1u</sub>	010100F <sub>1u</sub>	$0.1283(27) \times 10^{-4}$	
	2(2, 0E <sub>g</sub> )	010100F <sub>1u</sub>	010100F <sub>1u</sub>	$0.844(14) \times 10^{-5}$	
	2(2, 0F <sub>2g</sub> )	010100F <sub>1u</sub>	010100F <sub>1u</sub>	$-0.636(22) \times 10^{-5}$	
5	3(1, 0F <sub>1g</sub> )	010100F <sub>1u</sub>	010100F <sub>1u</sub>	$-0.207(37) \times 10^{-7}$	
	3(3, 0F <sub>1g</sub> )	010100F <sub>1u</sub>	010100F <sub>1u</sub>	$0.478(37) \times 10^{-7}$	
6	4(0, 0A <sub>1g</sub> )	010100F <sub>1u</sub>	010100F <sub>1u</sub>	$-0.179(33) \times 10^{-9b}$	
$v_2 = v_4 = 1: F_{1u}-F_{2u}$ interaction					
3	1(1, 0F <sub>1g</sub> )	010100F <sub>1u</sub>	010100F <sub>2u</sub>	$-0.684(13) \times 10^{-3}$	
4	2(2, 0E <sub>g</sub> )	010100F <sub>1u</sub>	010100F <sub>2u</sub>	0.0 <sup>a</sup>	
	2(2, 0F <sub>2g</sub> )	010100F <sub>1u</sub>	010100F <sub>2u</sub>	0.0 <sup>a</sup>	
5	3(1, 0F <sub>1g</sub> )	010100F <sub>1u</sub>	010100F <sub>2u</sub>	0.0 <sup>a</sup>	
	3(3, 0A <sub>2g</sub> )	010100F <sub>1u</sub>	010100F <sub>2u</sub>	$-0.48(14) \times 10^{-8}$	
	3(3, 0F <sub>1g</sub> )	010100F <sub>1u</sub>	010100F <sub>2u</sub>	0.0 <sup>a</sup>	
	3(3, 0F <sub>2g</sub> )	010100F <sub>1u</sub>	010100F <sub>2u</sub>	0.0 <sup>a</sup>	
$v_2 = v_4 = 1: F_{2u}$ sublevel					
2	0(0, 0A <sub>1g</sub> )	010100F <sub>2u</sub>	010100F <sub>2u</sub>	$-0.99525(52)$	
3	1(1, 0F <sub>1g</sub> )	010100F <sub>2u</sub>	010100F <sub>2u</sub>	$0.1842(27) \times 10^{-2}$	
4	2(0, 0A <sub>1g</sub> )	010100F <sub>2u</sub>	010100F <sub>2u</sub>	$-0.118(26) \times 10^{-4}$	
	2(2, 0E <sub>g</sub> )	010100F <sub>2u</sub>	010100F <sub>2u</sub>	$0.495(33) \times 10^{-5}$	
	2(2, 0F <sub>2g</sub> )	010100F <sub>2u</sub>	010100F <sub>2u</sub>	$-0.327(38) \times 10^{-5}$	
5	3(1, 0F <sub>1g</sub> )	010100F <sub>2u</sub>	010100F <sub>2u</sub>	$-0.294(22) \times 10^{-7}$	
	3(3, 0F <sub>1g</sub> )	010100F <sub>2u</sub>	010100F <sub>2u</sub>	$-0.234(15) \times 10^{-7}$	

759 data fitted,  $J_{\text{max}} = 112$ ,  $\sigma^c = 2.14 \times 10^{-3} \text{ cm}^{-1}$

Standard deviation is given in parentheses in the unit of the last two digits.

<sup>a</sup> Fixed parameter.

<sup>b</sup> Other parameters at this order are fixed to 0 and not indicated.

<sup>c</sup> Root mean square of  $v_{\text{obs.}} - v_{\text{calc.}}$

To calculate transition intensities for infrared absorption, the dipole moment operator is expanded using the same methods, as described in [18]. However, as we do not study here absolute intensities, this operator is developed up to the zeroth order only, and the corresponding parameter is simply set to 1.

We can finally notice that  $\nu_2 + \nu_4$  has two vibrational sublevels since

$$E_g \otimes F_{2u} = F_{1u} \oplus F_{2u}. \quad (7)$$

Only transitions from the ground state to the  $F_{1u}$  sublevel are allowed in a first approximation, since the dipole moment has  $F_{1u}$  symmetry in the molecule-fixed frame [18]. However, transitions to the  $F_{2u}$  sublevel appear due to strong interactions that mix the two sublevels, as we will see below.

#### 4. Analysis

The analysis of the  $\nu_2 + \nu_4$  combination bands takes advantage of the vibrational extrapolation concept illustrated in Eq. (6): the effective Hamiltonian contains contributions from the lower levels ( $GS$ ,  $\nu_2$ , and  $\nu_4$ ) which are known from previous studies [11,12,14]. The first step then consists in finding correct positions for the two sublevels. Initial simulations were performed by placing the “allowed”  $F_{1u}$  sublevel on the most prominent  $Q$  branch feature near  $1257 \text{ cm}^{-1}$  (see Fig. 2). The “forbidden”  $F_{2u}$  sublevel was then moved by hand until the simulation looks acceptable, at least for the lowest  $J$  values. It was then possible to assign many transitions.

The contributions of the  $GS$ ,  $\nu_2$ ,  $\nu_4$ , and  $\nu_2 + \nu_4$  to the final effective Hamiltonian were expanded up to orders 6, 3, 4, and 6, respectively.  $GS$ ,  $\nu_2$ , and  $\nu_4$  parameters were fixed to the values taken from [11, 12]. The spectrum is quite dense with many coalesced line clusters and is thus not very easy to assign in all parts. However, we could obtain a very satisfactory agreement using 759 assignments up to  $J = 112$ , which is quite a high-rotational excitation. Seventeen parameters from  $\nu_2 + \nu_4$  could be fitted, the others being fixed to zero. Only one 6-order (for the  $F_{1u}$  sublevel) and two  $F_{1u}$ – $F_{2u}$  interaction parameters have been used. The distance between the two vibrational sublevels is  $0.348 \text{ cm}^{-1}$ . Table 1 summarizes the results. Correspondence between our parameter notation and that of other authors for the  $GS$ ,  $\nu_2$ , and  $\nu_4$  can be found in previous papers [12,17]. The “usual notation” as been indicated only for the “main” parameters (band centers, rotational, and Coriolis constants) in the Table. As it can be seen in Figs. 2 and 3 the overall agreement is very good. It seems likely that many hot band lines also occur in the experimental spectrum. It was not possible to assign transitions arising from the minor sulfur isotopes.

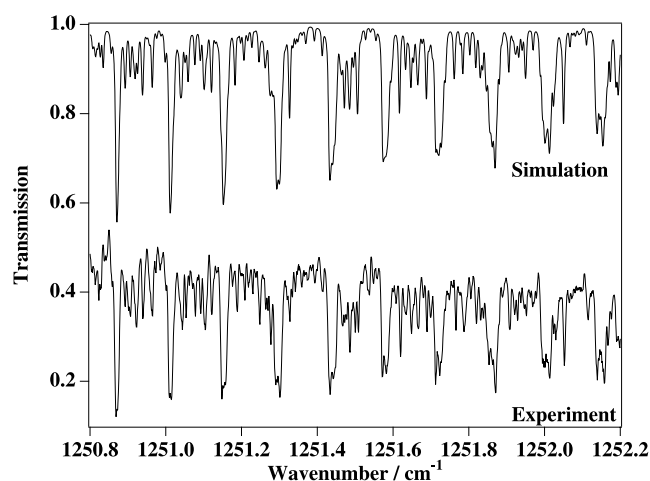


Fig. 3. Comparison between experimental and simulated spectra: detail in the  $P$  branches region.

The analysis has been performed using a non-linear least squares fit procedure included in the HTDS program suite dedicated to octahedral  $XY_6$  molecules [16] which has been recently updated to handle high- $J$  values (up to  $J = 199$ ).

Fig. 4 shows the “observed” and calculated reduced energy levels obtained by subtracting the scalar term, i.e.,

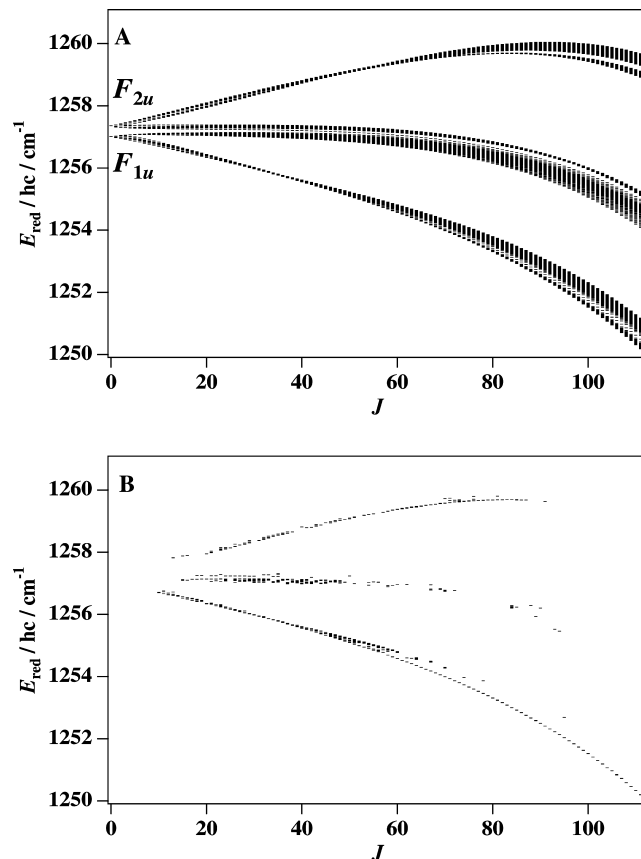


Fig. 4. Calculated (A) and observed (B) reduced energy levels (see text).

$$E_{\text{red}} = E - \sum_{\Omega} t_{\{0\}\{0\}}^{\Omega(0,0A_{1g})A_{1g}A_{1g}} (J(J+1))^{\Omega/2}$$

$$= E - B_0 J(J+1) + D_0 J^2 (J+1)^2 - \dots \quad (8)$$

The “observed” levels are those that are reached by observed transitions. We can see that they are relatively well distributed between the two sublevels. This means that we have in this way a correct sampling of the whole band.

## 5. Conclusion

We have presented here the first detailed analysis of the  $\nu_2 + \nu_4$  combination band of  $^{32}\text{SF}_6$ . Since the  $\nu_2$ ,  $\nu_2 + \nu_6$  [10,11],  $\nu_4$  and  $\nu_4 + \nu_6 - \nu_6$  [12] bands have already been analyzed separately, a further step could be a simultaneous fit of these four bands together with  $\nu_2 + \nu_4$ . This may improve the determination of the parameters for the lowest and forbidden  $\nu_6 = 1$  level which is responsible for many hot bands. Of course, one could think to include even more bands ( $\nu_3$ ,  $\nu_2 + \nu_3$ , ...) in order to perform a global fit of all the lowest  $\text{SF}_6$  vibrational levels.

The HTDS software [16] used to perform the present analysis can be freely downloaded though the World Wide Web at the URL: <http://www.u-bourgogne.fr/LPUB/shTDS.html>.

## Acknowledgments

Région Bourgogne is gratefully acknowledged for supporting the Laboratoire de Physique de l'Université de Bourgogne.

## References

- [1] T. Reddmann, R. Ruhnke, W. Kouker, J. Geophys. Res. 106 (D13) (2001) 14525–14537.
- [2] M. Khalil, Annu. Rev. Energy Environ. 24 (1999) 645–661.
- [3] C. Dervos, P. Vassiliou, Air Waste Manag. Assoc. 50 (2000) 137–141.
- [4] L. Geller, J. Elkins, J. Lobert, A. Clarke, D. Hurst, J. Butler, R. Myers, Geophys. Res. Lett. 24 (6) (1997) 675–678.
- [5] C. Volk, J. Elkins, D. Fahey, G. Dutton, J. Gilligan, M. Loewenstein, J. Podolske, K. Chan, M. Gunson, J. Geophys. Res. 102 (D21) (1997) 25543–25564.
- [6] J. Reilly, M. Mayer, J. Harnisch, Environ. Model. Assess. 7 (2002) 217–229.
- [7] J. Harnisch, N. Höhne, Environ. Sci. Pollut. Res. 9 (5) (2002) 315–320.
- [8] J. Harnisch, D. de Jager, J. Gale, O. Stobbe, Environ. Sci. Pollut. Res. 9 (6) (2002) 369–374.
- [9] V. Boudon, G. Pierre, Rovibrational spectroscopy of sulphur hexafluoride: a review, in: S.G. Pandalai (Ed.), Recent Research Developments in Molecular Spectroscopy, vol. 1, Transworld Research Network, Trivandrum, India, 2002, pp. 25–55.
- [10] V. Boudon, M. Hepp, M. Herman, I. Pak, G. Pierre, J. Mol. Spectrosc. 192 (1998) 359–367.
- [11] D. Bermejo, R. Martínez, E. Loubignac, V. Boudon, G. Pierre, J. Mol. Spectrosc. 201 (2000) 164–171.
- [12] V. Boudon, G. Pierre, H. Bürger, J. Mol. Spectrosc. 205 (2001) 304–311.
- [13] V. Boudon, D. Bermejo, J. Mol. Spectrosc. 213 (2002) 139–144.
- [14] O. Acef, C. Bordé, A. Clairon, G. Pierre, B. Sartakov, J. Mol. Spectrosc. 199 (2000) 188–204.
- [15] R. McDowell, B. Krohn, H. Flicker, M.C. Vasquez, Spectrochim. Acta A 42 (2/3) (1986) 351–369.
- [16] C. Wenger, V. Boudon, J.-P. Champion, G. Pierre, J. Quant. Spectrosc. Radiat. Transfer 66 (1) (2000) 1–16.
- [17] J.-P. Champion, M. Loëte, G. Pierre, Spherical top spectra, in: K.N. Rao, A. Weber (Eds.), Spectroscopy of the Earth's Atmosphere and Interstellar Medium, Academic Press, San Diego, 1992, pp. 339–422.
- [18] N. Cheblal, M. Loëte, V. Boudon, J. Mol. Spectrosc. 197 (1999) 222–231.